

Affimer reagents as tool molecules to modulate platelet GPVI-ligand interactions and specifically bind GPVI dimer

Rui-Gang Xu,¹ Christian Tiede,² Antonio N. Calabrese,² Lih T. Cheah,¹ Thomas L. Adams,² Julia S. Gauer,¹ Matthew S. Hindle,^{1,3} Beth A. Webb,¹ Daisie M. Yates,¹ Alexandre Slater,⁴ Cédric Duval,¹ Khalid M. Naseem,¹ Andrew B. Herr,⁵ Darren C. Tomlinson,² Steve P. Watson,⁴ and Robert A. S. Ariens¹

¹Discovery and Translational Science Department, Leeds Institute of Cardiovascular and Metabolic Medicine and ²Astbury Centre for Structural Molecular Biology and School of Molecular and Cellular Biology, Faculty of Biological Sciences, University of Leeds, Leeds, United Kingdom; ³Centre for Biomedical Science Research, School of Health, Leeds Beckett University, Leeds, United Kingdom; ⁴Institute of Cardiovascular Sciences, College of Medical and Dental Sciences, University of Birmingham, Birmingham, United Kingdom; and ⁵Division of Immunobiology and Division of Infectious Diseases, Cincinnati Children's Hospital Medical Center, Cincinnati, OH

Key Points

- We generated Affimers against platelet GPVI and mapped their binding sites, revealing functional regions regulating ligand binding.
- A dimeric epitope was identified on GPVI for Affimer D18, which specifically binds GPVI dimer through a 1:1 interaction.

Glycoprotein VI (GPVI) plays a key role in collagen-induced platelet aggregation. Affimers are engineered binding protein alternatives to antibodies. We screened and characterized GPVI-binding Affimers as novel tools to probe GPVI function. Among the positive clones, M17, D22, and D18 bound GPVI with the highest affinities (dissociation constant (K_D) in the nanomolar range). These Affimers inhibited GPVI-collagen-related peptide (CRP)-XL/collagen interactions, CRP-XL/collagen-induced platelet aggregation, and D22 also inhibited in vitro thrombus formation on a collagen surface under flow. D18 bound GPVI dimer but not monomer. GPVI binding was increased for D18 but not M17/D22 upon platelet activation by CRP-XL and adenosine 5'-diphosphate. D22 but not M17/D18 displaced nanobody 2 (Nb2) binding to GPVI, indicating similar epitopes for D22 with Nb2 but not for M17/D18. Mapping of binding sites revealed that D22 binds a site that overlaps with Nb2 on the D1 domain, whereas M17 targets a site on the D2 domain, overlapping in part with the glenzocimab binding site, a humanized GPVI antibody fragment antigen-binding fragment. D18 targets a new region on the D2 domain. We found that D18 is a stable noncovalent dimer and forms a stable complex with dimeric GPVI with 1:1 stoichiometry. Taken together, our data demonstrate that Affimers modulate GPVI-ligand interactions and bind different sites on GPVI D1/D2 domains. D18 is dimer-specific and could be used as a tool to detect GPVI dimerization or clustering in platelets. A dimeric epitope regulating ligand binding was identified on the GPVI D2 domain, which could be used for the development of novel bivalent antithrombotic agents selectively targeting GPVI dimer on platelets.

Introduction

Glycoprotein VI (GPVI) is a platelet receptor that plays important roles in hemostasis and pathological processes such as arterial and venous thrombosis.¹ Upon vascular trauma or atherosclerotic plaque rupture, GPVI interacts with the exposed subendothelial collagen, initiating a signaling cascade for platelet activation and blood clot formation² (supplemental Figure 1). Recent studies have indicated that GPVI also

Submitted 17 January 2024; accepted 27 May 2024; prepublished online on *Blood Advances* First Edition 14 June 2024; final version published online 25 July 2024.
<https://doi.org/10.1182/bloodadvances.2024012689>.

Raw HDX-MS data are available at ProteomeXchange Consortium via the PRIDE partner repository (data set identifier PXD046982).

Data are available on request from the corresponding author, Rui-Gang Xu (r.xu1@leeds.ac.uk).

The full-text version of this article contains a data supplement.

© 2024 by The American Society of Hematology. Licensed under [Creative Commons Attribution-NonCommercial-NoDerivatives 4.0 International \(CC BY-NC-ND 4.0\)](https://creativecommons.org/licenses/by-nc-nd/4.0/), permitting only noncommercial, nonderivative use with attribution. All other rights reserved.

supports thrombus growth via its interaction with fibrin.³⁻⁵ The GPVI extracellular region is composed of immunoglobulin-like domains D1 and D2. The collagen binding site is localized in D1⁶ (supplemental Figure 2A). Some studies have indicated a role for D2 in receptor dimerization.^{7,8} GPVI is expressed either as a mixture of monomers and dimers or predominantly monomers on resting platelets, with the binding of ligands, such as collagen and fibrin, inducing higher-order clustering and platelet signaling.⁹⁻¹¹ Dimerization of GPVI on platelets is stabilized through an intramolecular disulphide bond in the cytoplasmic region.¹² The number of GPVI dimers has been reported to increase upon platelet activation.^{9,10} Crystallographic studies have shown that GPVI can be either monomeric or dimeric.^{6-8,13,14} Despite data suggesting the existence of dimeric GPVI, GPVI extracellular domains associate with each other weakly, and no clear dimer formation has been observed in solution.^{7,15}

GPVI could be a promising drug target for novel antithrombotic molecules with a low bleeding risk.^{16,17} Understanding functional sites on GPVI that regulate GPVI-ligand interactions provides valuable information to help guide inhibitor design. Recently, 2 functional sites were identified on GPVI by structural studies using nanobodies (Nbs) and a fragment antigen-binding (Fab) fragment. The first is on the D1 domain, adjacent to the collagen-related peptide (CRP) binding site. Binding of Nb2 to this site allosterically inhibited collagen/CRP binding and platelet aggregation^{8,14} (supplemental Figure 2A). In the Nb2 bound crystal structure, GPVI adopts a D2 domain-swapped dimer conformation (supplemental Figure 2B). The domain swap is mediated by the C-C' hinge loop, possibly playing an important role in platelet signaling. The second functional site occupies a discontinuous region in the D2 domain and includes the C-C' hinge loop region. This site is targeted by glenzocimab, a humanized GPVI antibody Fab fragment that is under development at the clinical stage.¹³ It has been suggested that inhibition by glenzocimab blocks collagen binding through a combination of steric hindrance and allosteric changes. Inhibition of this site also affects GPVI dimerization and clustering.¹³

Affimers are engineered conformational binding proteins that possess many desirable properties of antibodies, including high specificity and high affinity binding, while additionally featuring substantial stability, simplicity, versatility, and cost-effective production.^{18,19} There are 2 types of Affimers, one based on the human stefin A protein and the second on a consensus plant cystatin sequence.^{19,20} Affimers present 2 variable regions of 9 residues for molecular recognition (supplemental Figure 3). Structurally, Affimers have an alpha helix positioned above an antiparallel beta sheet, which is different than the immunoglobulin fold in antibodies. Affimers are more stable than antibodies and easily modified to the needs of studying target protein function including the capability of intracellular expression.²¹ Affimers are isolated from a library comprising ~10⁶ sequences using phage display, which overcomes the costs/ethics associated with animals used for antibody production.^{22,23}

Here, we screened for Affimers targeting GPVI and characterized their effect on ligand interactions, platelet aggregation, and in vitro thrombus formation. We also mapped their binding sites on GPVI and compared binding to GPVI monomer vs dimer. Our data show that Affimers modulate GPVI function and bind different sites on GPVI. GPVI dimer can be specifically targeted by Affimer D18, thus representing a promising novel tool to further understand GPVI dimerization or clustering on platelets. A novel dimeric epitope is

identified on GPVI, representing a promising functional site for developing inhibitors selectively targeting GPVI dimer in platelets.

Methods

The main experimental methods used in this study include enzyme-linked immunosorbent assay (ELISA), microscale thermophoresis (MST), platelet aggregation assays, flow cytometry, in vitro thrombus formation assays, and native/hydrogen deuterium exchange mass spectrometry, which are briefly described below. For further details, please see the supplement. Other methods, including Affimer/GPVI expression and purification, surface plasmon resonance (SPR), pull-down assays, competition ELISA, biontination/fluorescent labeling of Affimer/GPVI, molecular modeling, platelet isolation, and blood collection, are described in the supplement.

ELISA was performed by incubating Affimers with immobilized GPVI-Fc on Maxisorp Nunc-immuno 96-well plates. Bound Affimers were detected using horseradish peroxidase conjugated rabbit anti-6-histag antibody (Cambridge Bioscience, Cambridge, United Kingdom). Data collection and analysis were performed as previously described.¹⁵

MST was carried out on a NT.115 (NanoTemper GmbH, Munich, Germany) instrument. Alexa Fluor 488 C5 maleimide-labeled Affimers were mixed with increasing concentrations of GPVI proteins. Data collection and analysis were performed as previously described.¹⁵

For platelet aggregation assays, washed platelets were incubated with Affimers at different concentrations for 15 minutes at 37°C. Aggregation was induced by CRP-XL or collagen and monitored using a Helena AggRAM (Helena Biosciences Europe, Tyne and Wear, United Kingdom).

For flow cytometry, washed platelets were incubated with Affimers conjugated to Alexa Fluor 488, CD42b⁻ allophycocyanin, with or without CRP-XL, or with or without adenosine 5'-diphosphate (ADP) for 20 minutes, followed by addition of 1% paraformaldehyde/phosphate-buffered saline volume-to-volume ratio (%) to halt the reaction.

In vitro thrombus formation assays were performed using Vena8 biochips (Cellix, Dublin, Ireland). Citrated human whole blood was incubated with 3,3'-dihexyloxycarbocyanine iodide for 10 minutes and perfused through collagen-coated microfluidic chips at 1000 per second for 2 minutes with or without GPVI Affimers. After flow, nonadherent platelets were washed off with phosphate-buffered saline for 3 minutes.

For native mass spectrometry, mixtures of GPVI proteins and Affimers were buffer exchanged into 0.2 M ammonium acetate (pH 6.9) before analysis.

Hydrogen deuterium exchange mass spectrometry (HDX-MS) was carried out using a liquid handling system (LEAP Technologies) coupled with an Acquity M-Class ultra-performance liquid chromatography/HDX manager (Waters). Samples were prepared by mixing GPVI proteins and Affimers in 10 mM potassium phosphate (pH 7.6). The HDX reactions were initiated by deuterated buffer and incubated at 4°C for 0.5 to 10 minutes. The reactions were then quenched, followed by proteolysis and peptide analysis.

Informed written consent was obtained for blood donations, according to the Declaration of Helsinki. Ethical approval was

obtained from the University of Leeds School of Medicine Research Ethics Committee (19-006).

Results

Screening of GPVI-targeting Affimers

Two-phase display screens against biotinylated recombinant GPVI monomer and dimer (supplemental Figure 4) were performed.

Purified Fc domain was screened in parallel to eliminate binders to this domain. After 3 rounds of panning, 2x24 colonies were tested for binding GPVI monomer and dimer by phage ELISA (Figure 1A-B). Sequencing revealed 17 unique binders from the GPVI monomer screen and 14 from the dimer screen. None of the binders interacted with the Fc domain (Figure 1A-B). In contrast to other Affimers that bound both monomer and dimer, Affimer D18 selectively bound GPVI dimer but not monomer. The Affimers were

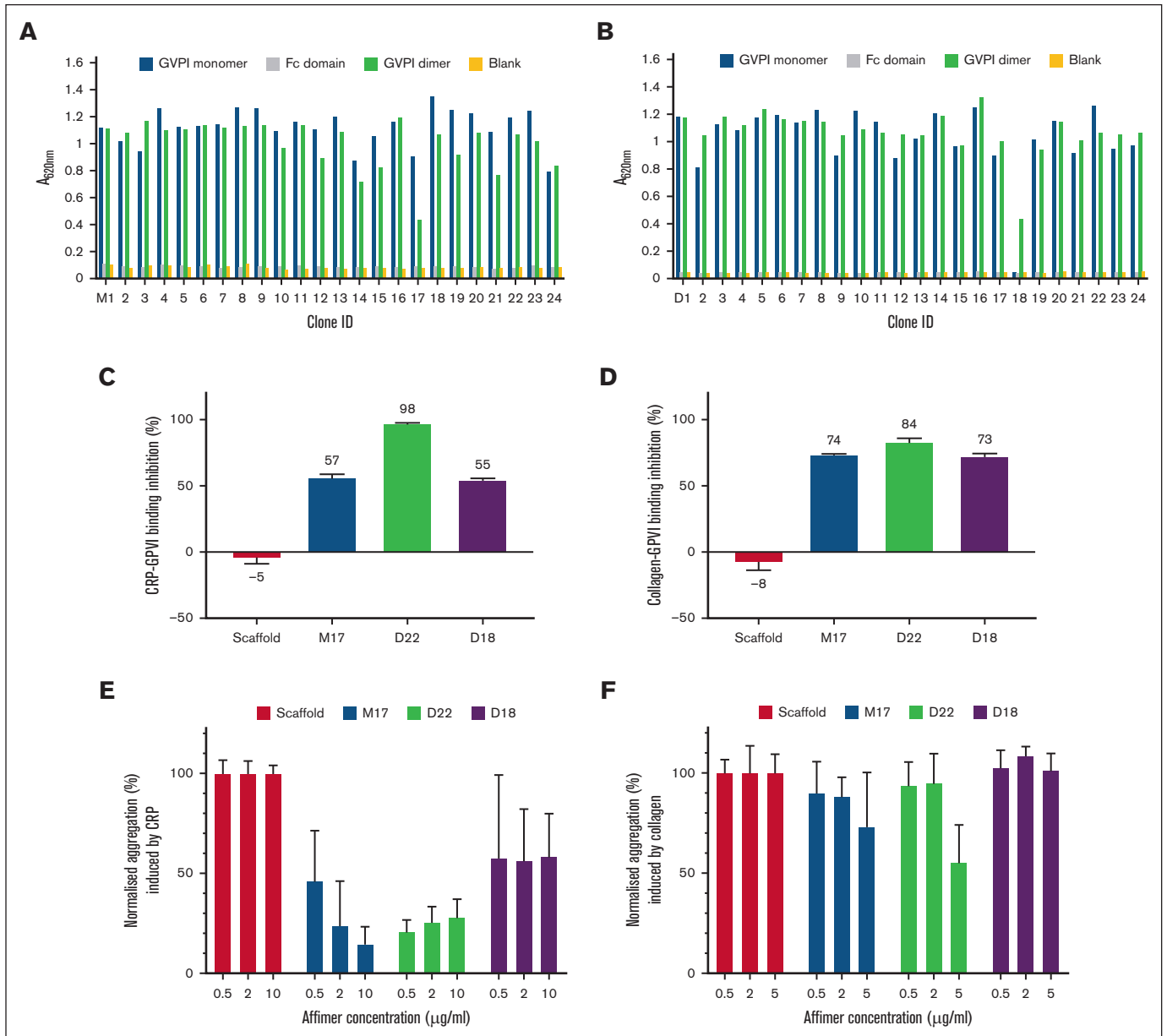


Figure 1. Identification of GPVI Affimers and their effect on GPVI-ligand interactions and platelet aggregation. Screening of GPVI-binding Affimers raised against GPVI monomer (A) and GPVI dimer (B) by phage ELISA. Fc domain (gray) was tested as a control. No protein was added in Blank (yellow). A total of 31 unique Affimers that bind to immobilized GPVI monomer (blue) and GPVI dimer (green) with the highest affinity were identified from 48 clones. These clones are numbered as M1 to M24 and D1 to D24 for Affimers screened against GPVI monomer and dimer, respectively. The effect of Affimers M17, D22, and the dimer-specific Affimer (D18) on GPVI dimer interaction with immobilized CRP-XL (C) and collagen (D) were characterized by competitive ELISA and expressed as % inhibition as compared to buffer control. Affimer scaffold was also used as a control. The effect of Affimers M17, D22 and D18 on CRP-XL (E) and collagen (F)-induced platelet aggregation was studied by aggregation assays. Data were normalized using the scaffold control (100% aggregation) as reference. Data are presented as mean ± standard deviation (SD); n ≥ 3.

subcloned and expressed in *Escherichia coli* and purified (supplemental Figure 5). Pull-down experiments were used to confirm Affimer interaction with GPVI. We selected 3 Affimers for further study based on pull-down experiments (data not shown) and binding affinity. The affinities of Affimers for GPVI were investigated by titrating Affimers over immobilized GPVI-Fc dimer using ELISA. Affimers, M17, D22, and D18 showed the highest affinities to GPVI dimer with K_{Ds} of 3.6 ± 0.2 nM, 13.0 ± 1.2 nM, and 0.14 ± 0.02 nM, respectively (supplemental Figure 6).

Effects of Affimers on GPVI-ligand interactions

Effects of Affimers on interactions of GPVI with collagen and CRP-XL were tested using competitive ELISAs. The Affimers inhibited GPVI interactions with CRP-XL and collagen to varying degrees (Figure 1C-D; supplemental Table 1). Among the 3 Affimers, D22 showed the strongest inhibition of GPVI interaction with both ligands, at 98% (CRP-XL) and 84% (collagen). Slightly weaker inhibition of GPVI interactions with CRP-XL and collagen was observed for M17 and D18 (57% and 55% for CRP-XL; 74% and 73% for collagen, respectively). These data show that Affimers modulate GPVI-ligand interactions.

Affimers modulate platelet aggregation

The effects of Affimers on platelet aggregation were characterized using light transmission aggregometry. CRP-XL and collagen were used to induce aggregation with or without preincubation with Affimers. Three agonist concentrations were tested to determine the optimal trigger (10 μ g/mL for CRP-XL and 5 μ g/mL for collagen) for aggregation (supplemental Figure 7). It has been reported that Fab fragments can trigger GPVI activation and platelet aggregation on their own.²⁴ To test the potential direct effect on platelet aggregation, Affimers were added to washed platelets, and the percentage of platelet aggregation without additional trigger was recorded. Negligible aggregation (<20%) was observed for M17, D22, and D18 (supplemental Figure 8). We next investigated the effect of Affimers on CRP-XL and collagen-mediated aggregation and found that Affimers M17 and D22 inhibited aggregation induced by both agonists (Figure 1E-F; Table 1; supplemental Table 1). Inhibition with D18 was only observed in CRP-XL but not collagen-induced aggregation at the tested Affimer concentrations. Stronger inhibition of platelet aggregation was observed for all Affimers when CRP-XL was used as agonist compared with collagen. The weaker inhibition when using collagen as agonist is likely due to the presence of receptor $\alpha 2\beta 1$, which has been reported to play a regulatory role in platelet activation by facilitating platelet-collagen but not CRP-XL adhesion.^{2,25} Similar observations have been observed for Nb2, in which

a much higher nanobody concentration was required to inhibit collagen but not CRP-XL-induced platelet aggregation.⁸ To confirm that Affimers are specific for GPVI, we found no effect of the Affimers on thrombin-induced platelet aggregation (supplemental Figure 9).

Affimers inhibit CRP-XL-GPVI binding with different efficacies

In our competition ELISA, D22 could almost fully inhibit CRP-XL binding to GPVI dimer, whereas M17 and D18 only partially inhibited the interaction (Figure 1C). The distinct inhibition effects for these Affimers suggest different inhibition mechanisms on CRP-XL binding. To further investigate this, we tested Affimers at multiple concentrations by competitive ELISA and determined their maximum inhibition efficacies. Consistent with our previous observations using a single Affimer concentration, we observed that although D22 had a maximum inhibition efficacy of 99%, M17 and D18 only partially inhibited the binding, with maximum efficacies of 69% and 61%, respectively (supplemental Figure 10).

Affimer D18 binds GPVI dimer but not monomer

Affimer D18 selectively bound GPVI dimer but not monomer in phage ELISA (clone 18, Figure 1B). To further investigate the selectivity of this Affimer, we developed an ELISA to analyze binding of D18 to immobilized GPVI monomer, dimer, and Fc domain. M17 and D22, which interacted with both GPVI monomer and dimer in the phage ELISA, were also tested. Consistent with the phage ELISA, M17 and D22 bound both monomer and dimer (supplemental Figure 11A-B), whereas D18 bound GPVI dimer but not monomer (supplemental Figure 11C). No binding was observed for the Affimer scaffold with either monomer or dimer of GPVI, and no GPVI-specific Affimer bound to the Fc domain (supplemental Figure 11A-C). The K_D of M17 binding to GPVI monomer and dimer was 11 ± 1 nM and 3.6 ± 0.2 nM, respectively (Figure 2A; Table 1; supplemental Table 2). D22 binds GPVI dimer at K_D of 13 ± 1 nM, whereas binding is not saturable with GPVI monomer, and a $K_D > 100$ nM (Affimer concentration that generates half of the maximum binding signal) was estimated from the data (Figure 2B; Table 1; supplemental Table 2). The K_D of D18 binding to GPVI dimer was 0.14 ± 0.02 nM, and no binding of D18 to GPVI monomer was observed at any Affimer concentration (Figure 2C; Table 1; supplemental Table 2). Affimer scaffold did not bind GPVI monomer or dimer (Figure 2A-C).

We next investigated the kinetics of the interactions of D18 with GPVI by SPR. GPVI monomer, dimer, and Fc domain were flowed over immobilized biotinylated D18 on a streptavidin chip, in comparison with M17 and D22. The K_D of M17 to GPVI monomer and

Table 1. Summary of the key properties of GPVI Affimers

Affimer	Binding sites on GPVI	K_D GPVI monomer, nM	K_D GPVI dimer, nM	Platelet aggregation (agonist: collagen/CRP)	Thrombus formation under flow (collagen surface)
M17	141Y-149T	55 ± 18	4.4 ± 4.3	↓/↓	–
D22	44S-53L	53 ± 11	5.3 ± 2.5	↓/↓	↓
D18	113Q-123F 141Y-149T	N.D.	0.23 ± 0.01	-/↓	–

Down arrow (↓) represents inhibition effect. Hyphen (-) represents no clear inhibition effect. K_D values were determined using SPR. N.D., not determinable.

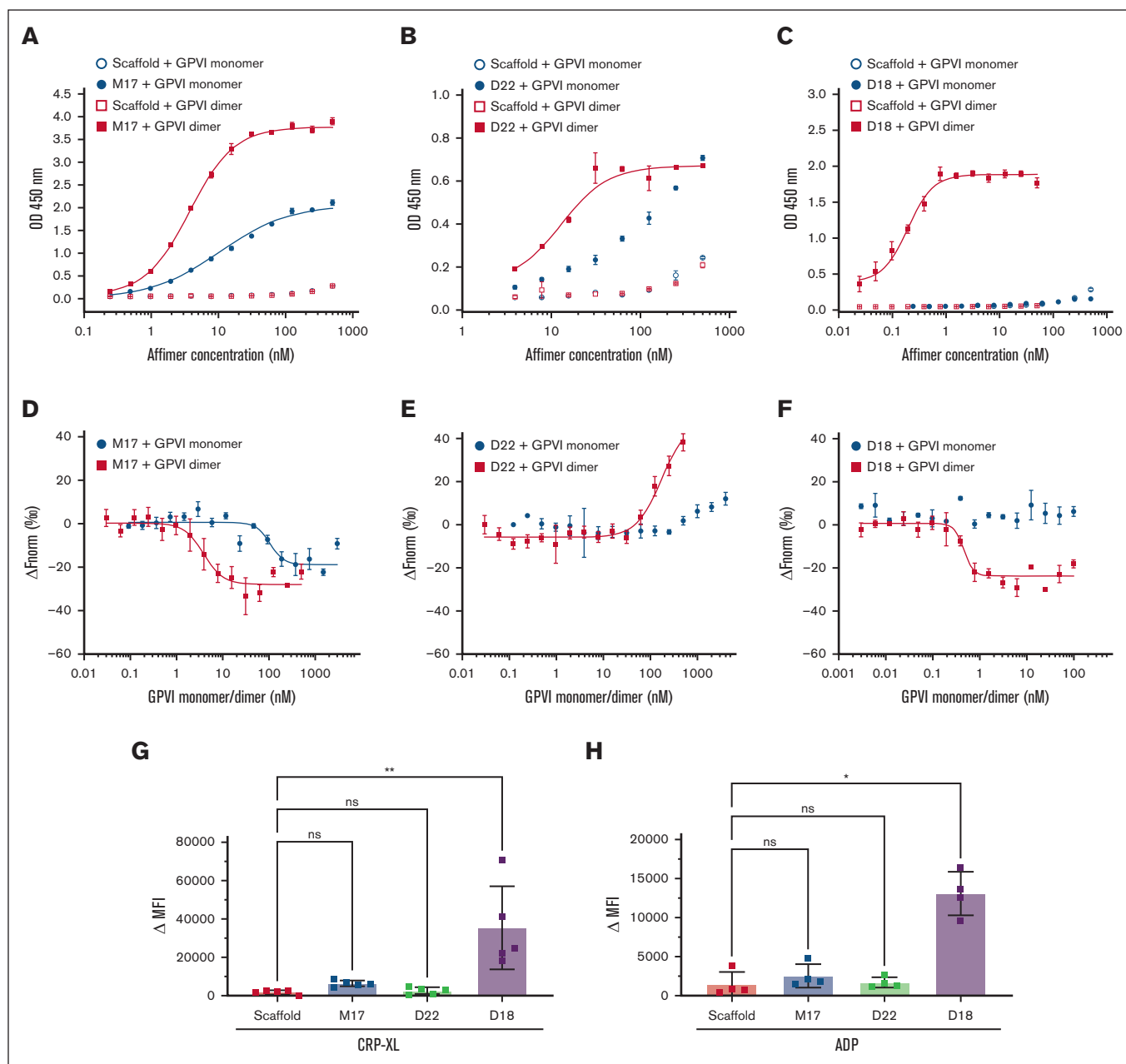


Figure 2. Interaction of Affimer M17, D22, and D18 with GPVI monomer and dimer analyzed by ELISA, MST, and flow cytometry. ELISA: (A) M17 bound GPVI monomer (blue circles) at K_D of 11 ± 1 nM, and GPVI dimer (red squares) at K_D of 3.6 ± 0.2 nM. (B) D22 bound GPVI monomer at K_D of 53 ± 11 nM, and GPVI dimer at K_D of 5.3 ± 2.5 nM. (C) No binding was observed for D18 and GPVI monomer. D18 bound GPVI dimer at K_D of 0.14 ± 0.02 nM. K_D values were obtained through fitting data with Hill equation. MST: (D) M17 bound GPVI monomer at K_D of 105 ± 31 nM and GPVI dimer at K_D of 4 ± 2 nM. (E) D22 bound GPVI monomer at K_D of 171 ± 36 nM and GPVI dimer at $K_D > 1 \mu\text{M}$. (F) D18 bound GPVI dimer at K_D of 0.5 ± 0.2 nM. No binding was observed for D18 to GPVI monomer. K_D values were obtained through fitting data with Hill equation. For ELISA and MST, data and K_D were presented as mean \pm SD; $n \geq 3$. Flow cytometry: binding of Alexa Fluor 488 labeled Affimers scaffold, M17, D22, and D18 to washed platelets was analyzed by comparing the mean fluorescence intensity before and after stimulation (Δ MFI) with CRP-XL (G) and ADP (H). D18, but not M17 and D22, bound to activated platelets. Friedman test is used to determine statistical significance ($P < .05$). Data were presented as mean \pm SD; $n \geq 4$.

dimer was 55 ± 18 nM and 4.4 ± 4.3 nM, respectively (supplemental Figure 12A-B; Table 1; supplemental Tables 2-3). The K_D of D22 to GPVI monomer and dimer was 53 ± 11 nM and 5.3 ± 2.5 nM, respectively (supplemental Figure 12C-D; Table 1; supplemental Tables 2-3). The K_D of D18 to GPVI dimer was 0.23 ± 0.01 nM, whereas no binding was detected for D18 to

GPVI monomer (supplemental Figure 12E-F; Table 1; supplemental Tables 2-3). No binding was observed for the Fc domain (supplemental Figure 13).

Then, we used MST to study whether selective binding of Affimer D18 to GPVI dimer is also observed in solution. M17 bound GPVI

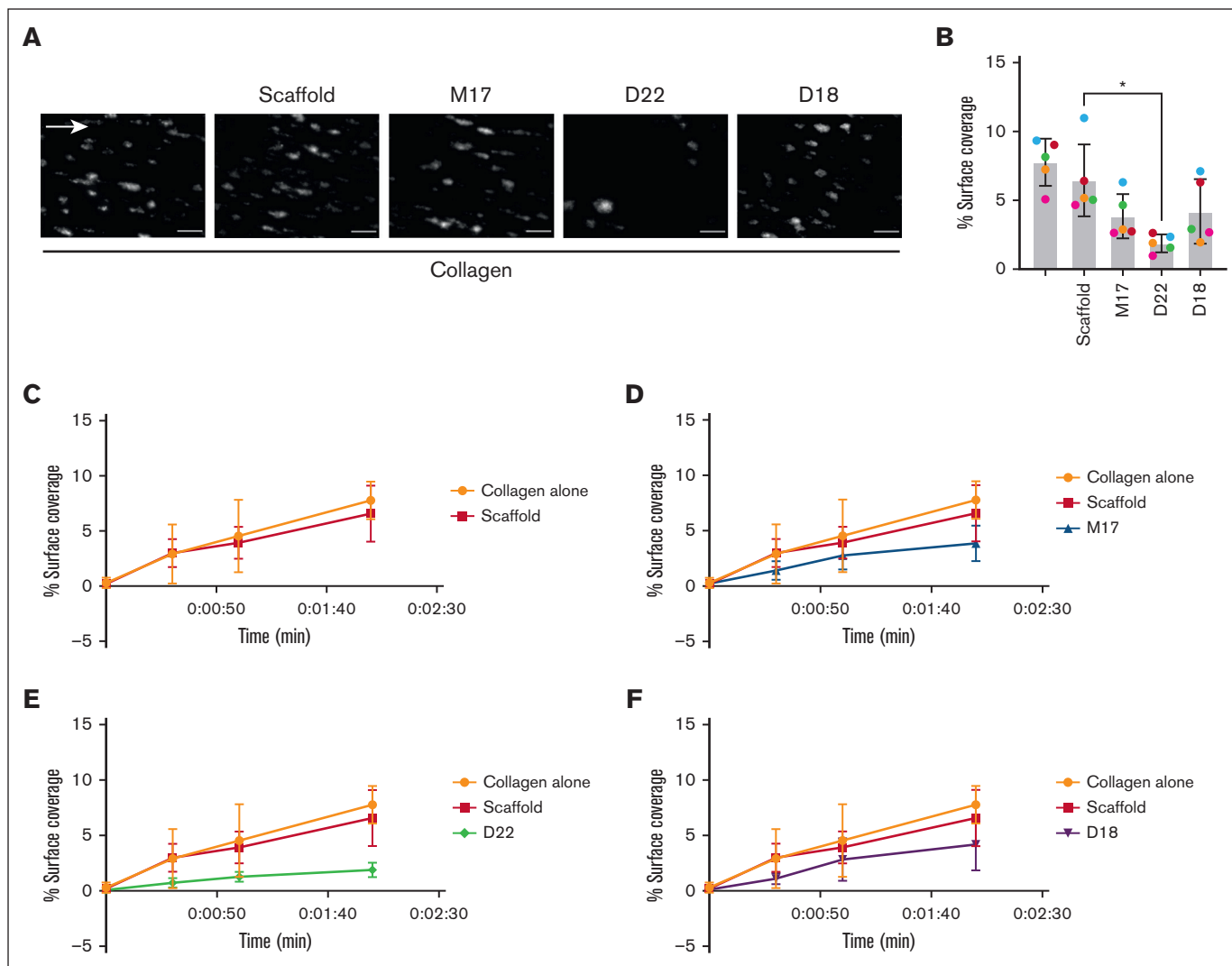


Figure 3. Effect of GPVI Affimers on thrombus formation in vitro. Human whole blood was incubated in the presence or absence of GPVI Affimers (Scaffold, M17, D22, and D18; 10 $\mu\text{g}/\text{mL}$) for 15 minutes and perfused through collagen (50 $\mu\text{g}/\text{mL}$) coated microfluidic chips at 1000 per second for 2 minutes. After 2 minutes of flow, nonadherent platelets were washed off with phosphate-buffered saline for 3 minutes. Images of stably adherent platelets and thrombi were taken by fluorescence microscopy and quantified using ImageJ. Data presented as representative images (scale = 20 μm) (A) and percentage surface coverage (B) at 2 minutes (repeated measures 1-way analysis of variance with Šidák multiple comparisons test vs scaffold; * $P < .05$). (C-F) Percentage surface coverage over time up to 2 minutes. Data presented as mean \pm SD; $n = 5$.

monomer and dimer in MST with K_D of 105 ± 31 nM and 4 ± 2 nM, respectively (Figure 2D; supplemental Table 2). D22 bound GPVI dimer in MST with K_D of 172 ± 31 nM. Binding did not reach saturation with GPVI monomer. The K_D was estimated at >1 μM (GPVI monomer concentration that generates half of the maximum binding signal) based on the data (Figure 2E; supplemental Table 2). D18 bound GPVI dimer at K_D of 0.5 ± 0.2 nM, whereas no D18 binding to GPVI monomer was observed (Figure 2F; supplemental Table 2). Taken together, the ELISA, SPR, and MST data show that D18 binds GPVI dimer selectively over monomer, and this occurs both in surface- and solution-based reactions.

Flow cytometry binding assays were then performed to study the (selective) binding of D18 to GPVI dimer on platelets. Washed platelets were activated by CRP-XL and ADP in the presence of

Alexa Fluor 488 labeled D18. Labeled M17, D22, and scaffold were also tested in parallel with D18. A significant increase of fluorescence was observed upon CRP-XL and ADP activation of the platelets for D18 binding compared with the scaffold, M17, and D22 (Figure 2G-H, supplemental Figure 14). These data indicate that D18 can bind GPVI dimers generated through GPVI clustering upon platelet activation with CRP-XL and ADP.

Affimers inhibit thrombus formation under flow

We next investigated the effects of Affimers on in vitro thrombus formation under flow conditions by flowing whole blood over a collagen-coated surface for 2 minutes, followed by a 3-minute buffer wash. The rationale for this setup is to allow for platelet adhesion for 2 minutes as per manufacturer instructions for the Cellix VenaFlux system and to ensure platelets are stably adhered

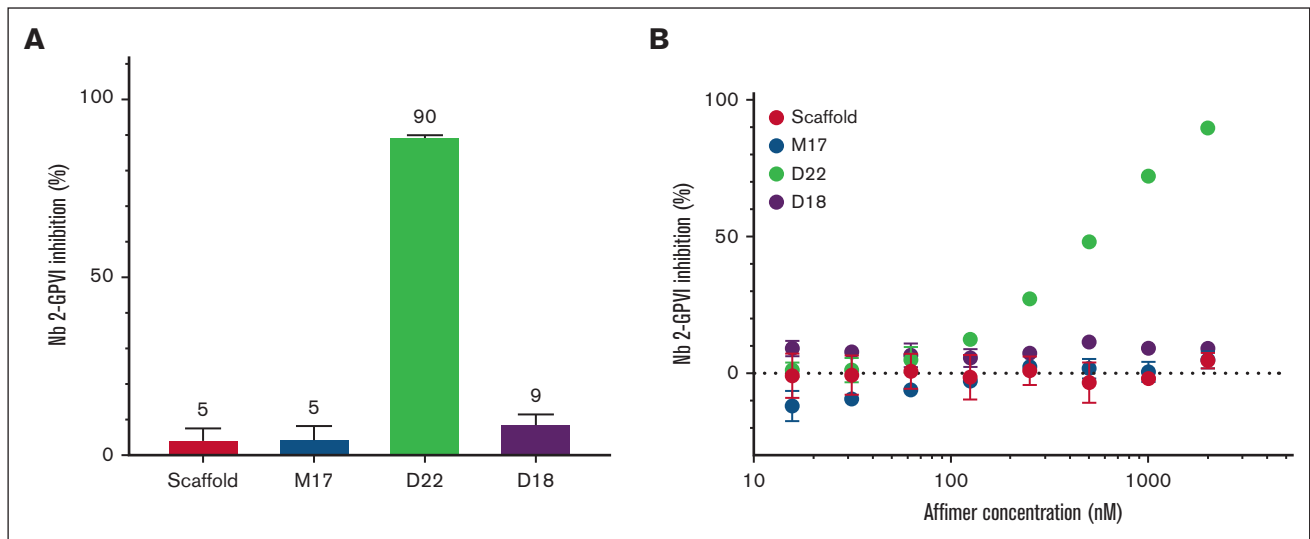


Figure 4. Competition of Affimers with Nb2 for GPVI dimer binding. (A) Displacement of Affimers by Nb2-GPVI dimer binding in competition ELISA. Affimers M17, D22, and D18 (2 μ M) were incubated with 100 nM Nb2 before the addition to immobilized GPVI dimer. (B) Effect of Affimers at multiple concentrations on Nb2-GPVI dimer binding. Affimer scaffold was used as control. Data were presented as mean \pm SD; n = 3.

after 2 minutes using a 3-minute buffer wash.^{26,27} Fluorescent images after 2 minutes of blood flow showed less thrombus formation only in the presence of Affimer D22 compared with buffer or scaffold controls (Figure 3A). Thrombus surface coverage was quantified and compared at all time points before 2 minutes (Figure 3B-F; Table 1). At 2 minutes, a significant reduction in mean surface coverage was only observed with D22 (1.8%) but not in the presence of M17 (3.8%) or D18 (4.1%) compared with buffer or scaffold controls (7.8% and 6.5%, respectively; Figure 3B). These data show that Affimers D22 inhibit thrombus formation under flow.

Competition of Affimers with Nb2 for GPVI

Slater et al recently reported that GPVI Nb2 binds GPVI in the D1 domain, supported by a new GPVI-Nb2 crystal structure.⁸ To investigate where Affimers bind GPVI in relation to Nb2, we performed competition ELISA by adding Nb2 with Affimers present on immobilized GPVI dimer. At a molar ratio of 20:1 (Affimer:Nb2), we observed strong inhibition by Affimer D22 (90%) on Nb2-GPVI interaction (Figure 4A). These effects were concentration dependent (Figure 4B). No inhibition was found for M17 and D18 (Figure 4A-B). These data indicate that although binding sites of D22 may have some overlap with the Nb2 site, M17 and D18 bind to distinct sites compared with the Nb2 site on GPVI.

Affimer binding sites on GPVI

To pinpoint the location where Affimers bind on GPVI, we performed HDX-MS²⁸ on Affimers M17, D22, and the dimer-specific Affimer, D18. Several GPVI regions showed strong protection from deuterium exchange upon Affimer binding, including 141Tyr-149Thr on the D2 domain for M17 (Figure 5A; Table 1) and 44Ser-53Leu on the D1 domain for D22 (Figure 5B; Table 1). For D18, the protected region included 113Gln-123Phe and, to a lesser extent, 141Tyr-149Thr on the D2 domain (Figure 5C; Table 1). The regions with the strongest protection indicate key interacting sites

on GPVI for the Affimers. Binding of M17 led to deprotection of 86Val-112Leu on GPVI, indicating allosteric conformational changes upon M17 binding, resulting in destabilization of the hydrogen bonding network and increased flexibility of these regions. Our data suggest that 141Tyr-149Thr is a common site for binding of both M17 and D18. To further investigate the degree of overlap in this region, we performed a competition ELISA of D18 and M17 binding to GPVI. We observed a modest displacement of M17-GPVI interaction by D18 (24%), compared with scaffold (-2%) and D22 (-8%) controls, suggesting their binding sites in this region are partially overlapping (supplemental Figure 15). Together, the HDX-MS data identified key GPVI binding sites for M17, D22, and D18 and an allosteric site upon M17 binding.

The Affimer binding sites were compared with CRP, Nb2, and glenzocimab sites on GPVI (Figure 5D). We observed that Affimer D22 site overlaps in part with the CRP and Nb2 sites on GPVI D1 domain. Tyr47, involved in both Nb2 and CRP binding, also forms part of the D22 binding site on GPVI D1 domain (supplemental Figure 2A). The binding site of Affimer M17, 141Tyr-149Thr, includes part of the glenzocimab site on GPVI D2 domain (144Ala-149Leu). No overlap was found for the major binding site of D18 on GPVI, 113Gln-123Phe, for all 3 ligands. Thus, although the binding sites for D22 and M17 show some degree of overlap with the sites for Nb2 and glenzocimab on GPVI, respectively, D18 largely interacts with a new region on GPVI that does not overlap with any of these known sites.

Affimer D18 is a stable dimer

To further understand how dimer-specific Affimer D18 interacts with GPVI dimer, the stoichiometry of this interaction was determined by native mass spectrometry. We observed that D18 was a stable dimer on its own. M17, which was tested as a control, was predominantly monomeric (Figure 6A; supplemental Figure 16). This observation is consistent with the larger predicted molecular weight from a calibrated size exclusion column compared with its

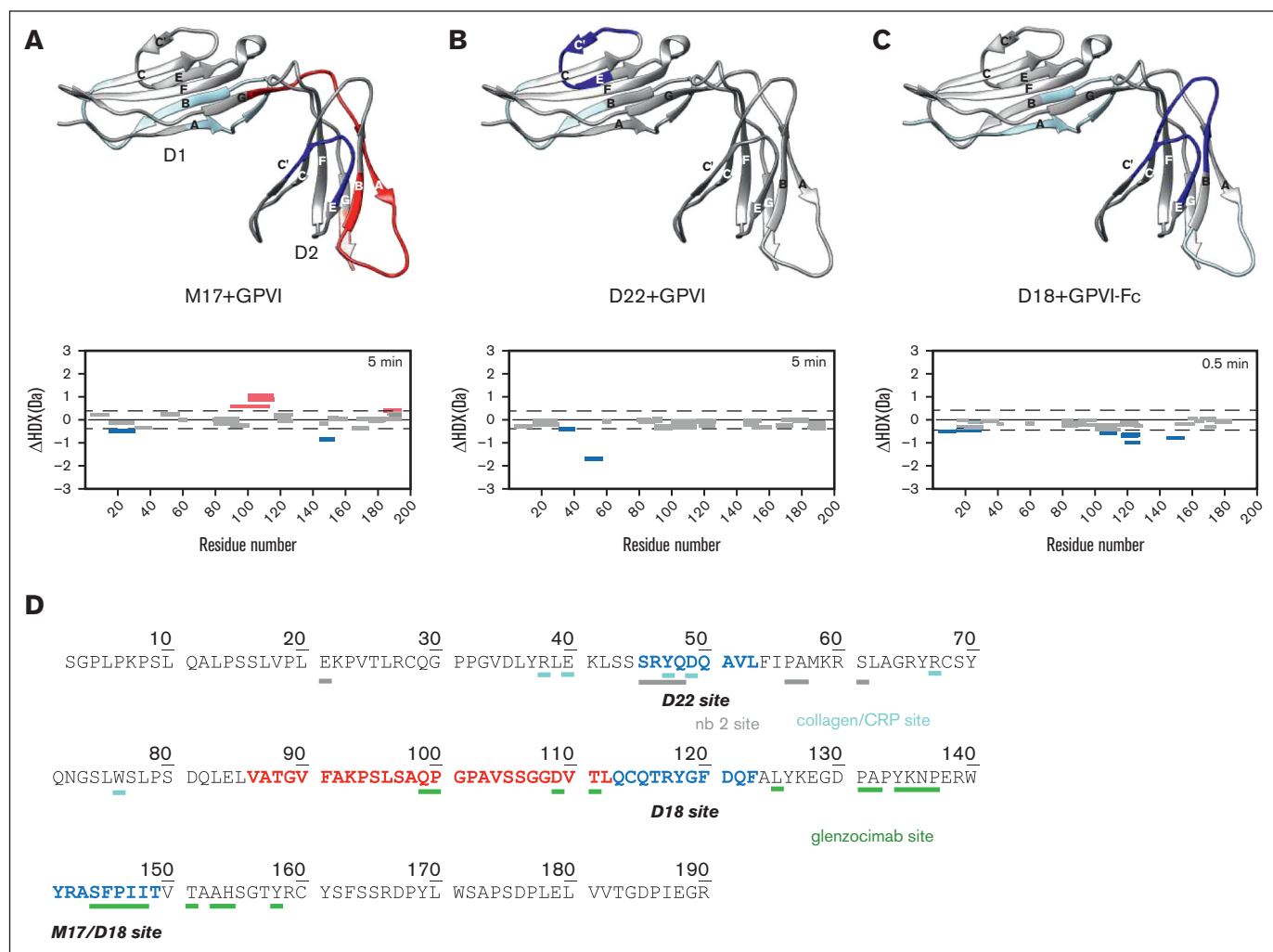


Figure 5. The location of Affimer binding sites on GPVI for M17, D22, and D18. The residues involved in Affimer binding on GPVI determined by HDX-MS for M17 (A), D22 (B), and D18 (C) are displayed and colored on the crystal structure of GPVI (gray, PDB code: 2GI7). The residues that had strong and weak protection effect upon Affimer binding are colored blue and light blue, respectively. The residues that had strong and weak deprotection effect upon Affimer binding are colored red and light red, respectively. Red, blue, and gray bars shown in each graph below the GPVI structure represent different GPVI peptide fragments generated by proteolysis in the presence and absence of Affimers. The peptide fragment represented by red and blue bars have positive and negative differences in deuterium uptake, respectively. The peptide fragments represented by gray bars have no significant changes in deuterium uptake. (D) Representation and comparison of the binding site residues of M17, D22, and D18 with collagen/CRP (cyan), glenzocimab (green) and Nb2 (gray). The amino acids colored in blue and red had the strong protection and deprotection effect, respectively, upon the binding of Affimers.

theoretical monomeric weight and when compared with M17 (supplemental Figure 17). We next investigated whether D18 forms stable complexes with GPVI monomer and dimer. To minimize the interference of glycosylation in molecular weight determination, a variant of GPVI (N72Q) that does not undergo glycosylation were used in the experiment.⁸ We found that no complex formation was observed in a 1:1 molar ratio solution of D18 with GPVI (Figure 6B-C). Stable complex formation was, however, detected when D18 was added to GPVI-Fc dimer using the same experimental conditions. When GPVI dimer was added to D18 at 1:1 molar ratio, complex formation was observed. The molecular weight of the complex corresponds to 1 GPVI dimer interacting with 1 D18 dimer (1:1 complex). (Figure 6D-E). These data confirm that D18 is a stable dimer and specifically binds GPVI dimer but not monomer.

Modeling of GPVI-Affimer interactions

To further analyze how Affimers interact with GPVI at the molecular level, we modeled Affimers M17, D22, and D18 and their interactions with GPVI using high ambiguity driven protein-protein docking.²⁹ Residues in the variable loops of Affimers, and those in GPVI identified by HDX-MS, were used as active residues in the docking. For all models generated, the best scoring structure from the top cluster, with the lowest energy was selected. The molecular model for Affimers used in the docking were generated by AlphaFold³⁰ (Figure 6F). When the M17-GPVI model (Figure 6G) was superposed with glenzocimab-GPVI complex, we observed that the 2 variable loops of M17 were between the CDR loops of the heavy and light chains of glenzocimab (supplemental Figure 18A). To investigate the possible mechanisms for M17 inhibition on CRP-GPVI binding, we modeled CRP-XL to the M17-GPVI model by

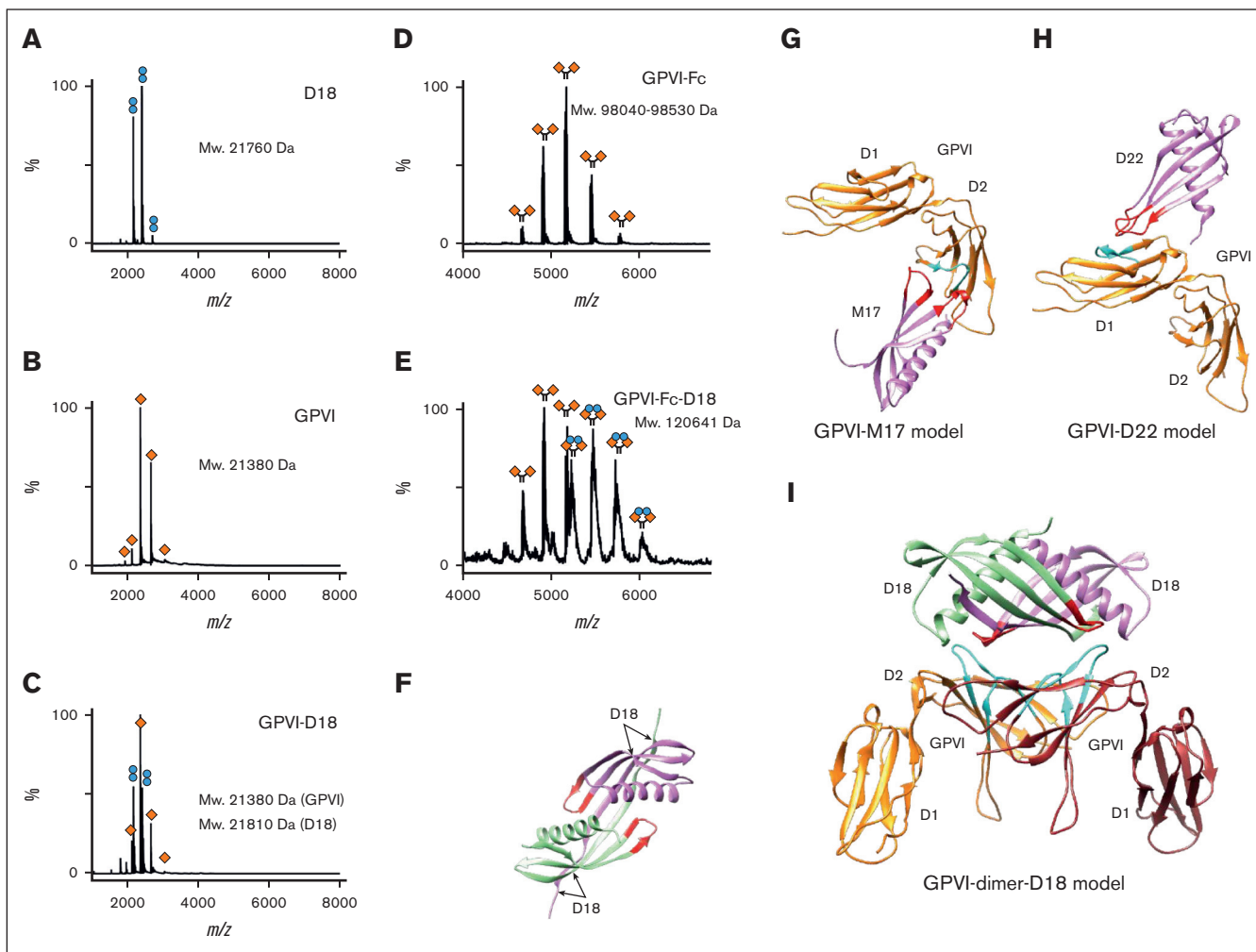


Figure 6. Characterization of GPVI-Affimer complexes by native mass spectrometry and molecular modeling. (A-E) The native mass spectra of D18 (dimeric, measured molecular weight is at 21 760 Da, approximately two-fold larger than that calculated based on the monomeric protein sequence, at 11 013 Da) (A), GPVI monomer N72Q (monomeric, measured molecular weight is at 21 380 Da, similar to that based on the monomeric protein sequence, at 21 249 Da) (B), GPVI monomer N72Q with D18 (no complex formation detected, measured molecular weight is at 21 380 and 21 810 Da for GPVI and D18, respectively) (C), GPVI-Fc N72Q (monomeric, measured molecular weight is at 98 040 to 98 530 Da due to heterogeneous glycosylation in Fc, similar to that based on the sequence of the monomeric protein, at 95 154 Da) (D), and GPVI-Fc N72Q with D18 (1:1 complex formation detected, measured molecular weight is at 120 641 Da, similar to that based on the protein sequence of the 1:1 complex, at 117 181 Da) (E). Orange diamonds and blue spheres represent GPVI and Affimer D18, respectively. (F) Molecular model of D18 dimer generated using AlphaFold. Molecular docking model of M17 (G), D22 (H), and D18 (I) interacting with GPVI generated using high ambiguity driven protein-protein docking. GPVI is colored in orange and brown. The regions interacting with Affimers predicted by HDX-MS are colored in cyan. Affimers are colored in magenta and green. The variable loops that are crucial for interacting with GPVI are colored in red.

structure superposition with the CRP bound GPVI structure. We observed that, unlike that reported for glenzocimab, bound CRP did not cause steric hindrance of M17 binding (supplemental Figure 18B-C). Superposition of the D22-GPVI model (Figure 6H) with the Nb2-GPVI complex showed that D22 occupies the same location as Nb2. The 2 variable loops of D22 were in close proximity with the CDRs of Nb2 (supplemental Figure 18D). Before the generation of a D18-GPVI model, using HDX-MS, we confirmed that residues in the variable loop region of Affimer D18 are involved in GPVI dimer binding (supplemental Figure 19). In the D18-GPVI model (Figure 6I; supplemental Figure 20), dimeric D18 interacts with the D2 domains from 2 symmetrically arranged GPVI molecules. The major and minor D18 binding regions on GPVI, 113Gln-123Phe and 144Ala-149Leu,

respectively, form a large binding surface and are close to the variable loops in D18. Together, these docking data provide structural insights into the molecular arrangements of the GPVI/Affimer complexes (Figure 6F-I; supplemental Figure 20; supplemental Figure 21).

Discussion

This study shows that GPVI-CRP-XL/collagen interaction and GPVI-mediated platelet aggregation can be modulated by Affimers. Effects of Affimers on the binding of GPVI to fibrin were not probed, which is a limitation of our study. Affimer D22 reduced thrombus formation in whole blood under in vitro flow conditions. The binding sites for Affimers M17, D22, and D18 on GPVI were

characterized and shown to represent several functional hot spots that could play important roles in regulating GPVI-ligand binding. Furthermore, we show that D18 is a stable dimer that binds selectively to GPVI dimer with subnanomolar affinity. D18 also selectively interacts with GPVI dimer generated by CRP-XL/ADP activation on platelets. These findings imply that D18 can specifically recognize GPVI dimer and thus serve as a promising tool to selectively detect GPVI dimerization or clustering in platelets.

The configuration of GPVI on resting platelets has been a topic of debate for many years, reported either as predominantly monomer⁹ or as a mixture of monomer and dimer.^{10,31} Other studies suggest a key role for GPVI clustering in platelet function.³² It has been reported that the expression level of GPVI dimers was increased in patients with stroke and obesity.^{33,34} A higher GPVI dimer level in patients was associated with higher platelet aggregation and P-selectin exposure in response to GPVI-specific agonists or measured by a dimer-specific antibody compared with healthy controls,^{9,33,34} suggesting that the GPVI dimer could be a potential biomarker and/or an antithrombotic target. Antibodies and Fabs that specifically recognize GPVI dimer have been previously reported.³⁵⁻³⁷ Nevertheless, the location of these dimer-specific sites on GPVI have not been identified. Using the dimer-specific Affimer D18, the dimeric epitope on GPVI was revealed for the first time, which could be informative for the design of novel antithrombotic agents specifically targeting GPVI dimer.

Our data show that Affimer D18 is a stable dimer itself. Similar Affimer dimers have been reported previously, including those targeting lysine linked di-ubiquitins. These Affimers bind di-ubiquitins at high affinity accompanied by slow off rate, whereas a much-reduced binding was observed for monoubiquitins.³⁸ Structural and biochemical data suggested that linked di-ubiquitins are conformationally flexible and can adopt distinct conformations in solution, and Affimer dimers can select and recognize a suitable dimer conformation from the population of conformations that they can adopt.³⁹ This is reminiscent of our observations for the D18 dimer that specifically binds GPVI dimer, either linked artificially by Fc domain or on the platelet surface, at high affinity ($K_D = 0.2 \pm 0.01$ nM) with slow off rate ($1.3 \pm 0.04 \times 10^{-4}$ s⁻¹), whereas negligible binding is observed for the monomer. Based on the above observations, it is possible that the conformational selection mechanism as suggested for Affimers dimers and linked di-ubiquitins may also apply for D18 dimer and GPVI dimer interaction.

Our D18-GPVI dimer model reveals a distinct dimeric arrangement of 2 GPVIs not observed in previous crystallographic studies. The dimer interface is formed by the β C'-E, A-B/F-G loops, and β C regions of the D2 domain (supplemental Figure 21C). Each D18 dimer subunit interacts with the identified residues in each GPVI dimer subunit through the variable loop. This is different to that of the back-to-back and domain-swapped dimer structures (2GI7, 5OU7, and 7NMU), in which GPVI either interacts with each other through the C-terminal β strand of the D2 domain (β G) (back-to-back)^{6,7} or through the β G of D2 domain and β E-F strands of the D1 domain (domain swap).⁸

Although the binding site for M17 on GPVI overlaps in part with the glenzocimab site, our structure comparisons show that binding of M17 to GPVI is unlikely to cause potential steric hindrance on CRP binding.¹³ The much smaller size of Affimers compared with Fab fragments (12 vs 50 kDa, respectively) may account for the

absence of potential steric hindrance in the inhibition. Moreover, M17 does not interact with the C-C' loop, which is the major binding site for glenzocimab. These observations suggest that M17 may use a different mechanism to inhibit CRP-GPVI binding compared with glenzocimab. Furthermore, our HDX-MS data suggest that M17-GPVI binding generates a conformational change in the D1-D2 hinge region. Our competition ELISA data show that M17 inhibits CRP binding with a much lower efficacy than that observed for D22, which fully inhibits the binding. These data imply that M17 is likely an allosteric inhibitor that partially inhibits CRP binding on D1 domain through conformational changes generated when binding to the distal D2 domain. Similar allosteric changes at the D1-D2 hinge region have not been observed for glenzocimab in the crystal structure. Further studies are needed to understand how allosteric changes of GPVI generate a partial inhibitory effect of M17 on ligand binding.

Our HDX-MS data show that D22 bound GPVI at a similar site as Nb2. Interestingly, we did not observe deprotection effect on the C-C' loop, suggesting that D22 binding to GPVI should not induce a conformation change in the C-C' loop. This also suggests that the domain-swapped GPVI dimer observed in the crystal structure of the Nb2-GPVI complex⁸ may not exist for the D22-GPVI complex in solution. It is possible that the formation of domain-swapped GPVI dimer with bound Nb2 is induced by conditions during the crystallization process or by differences between nanobody and Affimer binding to GPVI. Further work is needed to investigate whether this domain-swapped dimer is physiologically relevant.

In conclusion, we show that Affimers modulate GPVI interaction with collagen/CRP-XL and inhibit CRP-XL and collagen-mediated platelet aggregation by GPVI. We observed that Affimers M17, D22, and D18 bind to different sites on GPVI. Using HDX-MS, the Affimers' binding sites on GPVI revealed several regions that play important roles in regulating ligand binding. D22 inhibited *in vitro* thrombus formation. Moreover, we found that Affimer D18 selectively binds GPVI dimer but not monomer in platelets, thus representing a promising tool to further understand the role of the GPVI dimerization and clustering in platelet function. Finally, we show that D18 is a stable dimer that forms a 1:1 complex with GPVI dimer. A dimeric epitope on the D2 domain was found that could be used as a promising site for designing antithrombotic agents that specifically bind GPVI dimer.

Acknowledgments

This work was supported by a joint Wellcome Trust Investigator Award (204951/B/16/Z; S.P.W. and R.A.S.A.). R.-G.X. and R.A.S.A. were further supported by the Biotechnology and Biological Sciences Research Council (BBSRC) (BB/W000237/1). SPR and MST binding assays were performed in the Biomolecular Interactions facility, Astbury Centre for Structural Molecular Biology, Faculty of Biological Sciences, University of Leeds (partly funded by the Wellcome Trust 062164/Z00/Z). S.P.W. holds a British Heart Foundation Chair (03/003). A.N.C. acknowledges support of the Sir Henry Dale Fellowship jointly funded by the Wellcome Trust and the Royal Society (grant number 220628/Z/20/Z) and the support of a University Academic Fellowship from the University of Leeds. The R.A.S.A. laboratory is further supported in part by the National Institute for Health and Care Research (NIHR) Leeds Biomedical Research Centre. Funding

from BBSRC (BB/M012573/1) and the Wellcome Trust (208385/Z/17/Z) enabled the purchase of mass spectrometry equipment.

The views expressed are those of the author(s) and not necessarily those of the National Health Service, NIHR, or the Department of Health and Social Care.

Authorship

Contribution: R.-G.X. performed ELISA, SPR assays, MST assays, and molecular modeling/docking experiments, produced and characterized Affimers, purified GPVI proteins, and wrote and edited the manuscript; C.T. performed phage display screening; A.N.C. performed HDX/native-MS experiment; L.T.C., R.-G.X., and J.S.G. performed platelet aggregation assays; T.L.A. performed Affimer subcloning and pull-down assays; J.S.G. performed expression of the GPVI-Fc protein; M.S.H. and D.M.Y. performed flow cytometry experiment; B.A.W. performed thrombus formation assays; A.S. provided Nb2; C.D., K.M.N., D.C.T., and S.P.W. contributed to study design; R.A.S.A. conceived the study,

supervised the work, generated the funding, and edited the manuscript; and all authors read and approved the manuscript.

Conflict-of-interest disclosure: S.P.W. and A.S. have a patent for the anti-GPVI nanobodies (WO2022/136457). The remaining authors declare no competing financial interests.

ORCID profiles: R.-G.X., 0000-0003-0774-112X; C.T., 0000-0003-0280-4005; A.N.C., 0000-0003-2437-7761; T.L.A., 0000-0002-6539-0754; J.S.G., 0000-0002-0835-639X; M.S.H., 0000-0002-5633-2034; B.A.W., 0000-0001-9075-8250; D.M.Y., 0000-0001-7566-1653; A.S., 0000-0001-7166-438X; C.D., 0000-0002-4870-6542; D.C.T., 0000-0003-4134-7484; S.P.W., 0000-0002-7846-7423; R.A.S.A., 0000-0002-6310-5745.

Correspondence: Robert A. S. Ariëns, Leeds Institute of Cardiovascular and Metabolic Medicine, University of Leeds, Clarendon Way, Leeds LS2 9NL, United Kingdom; email: r.a.ariens@leeds.ac.uk; and Rui-Gang Xu, Leeds Institute of Cardiovascular and Metabolic Medicine, University of Leeds, Clarendon Way, Leeds LS2 9NL, United Kingdom; email: r.xu1@leeds.ac.uk.

References

1. Rayes J, Watson SP, Nieswandt B. Functional significance of the platelet immune receptors GPVI and CLEC-2. *J Clin Invest*. 2019;129(1):12-23.
2. Nieswandt B, Watson SP. Platelet-collagen interaction: is GPVI the central receptor? *Blood*. 2003;102(2):449-461.
3. Onselae M-B, Hardy AT, Wilson C, et al. Fibrin and D-dimer bind to monomeric GPVI. *Blood Adv*. 2017;1(19):1495-1504.
4. Mangin PH, Onselae M-B, Receveur N, et al. Immobilized fibrinogen activates human platelets through glycoprotein VI. *Haematologica*. 2018;103(5):898-907.
5. Induruwa I, Moroi M, Bonna A, et al. Platelet collagen receptor glycoprotein VI-dimer recognizes fibrinogen and fibrin through their D-domains, contributing to platelet adhesion and activation during thrombus formation. *J Thromb Haemost*. 2018;16(2):389-404.
6. Feitsma LJ, Brondijk HC, Jarvis GE, et al. Structural insights into collagen binding by platelet receptor glycoprotein VI. *Blood*. 2022;139(20):3087-3098.
7. Horii K, Kahn ML, Herr AB. Structural basis for platelet collagen responses by the immune-type receptor glycoprotein VI. *Blood*. 2006;108(3):936-942.
8. Slater A, Di Y, Clark JC, et al. Structural characterization of a novel GPVI-nanobody complex reveals a biologically active domain-swapped GPVI dimer. *Blood*. 2021;137(24):3443-3453.
9. Loyau S, Dumont B, Ollivier V, et al. Platelet glycoprotein VI dimerization, an active process inducing receptor competence, is an indicator of platelet reactivity. *Arterioscler Thromb Vasc Biol*. 2012;32(3):778-785.
10. Jung SM, Moroi M, Soejima K, et al. Constitutive dimerization of glycoprotein VI (GPVI) in resting platelets is essential for binding to collagen and activation in flowing blood. *J Biol Chem*. 2012;287(35):30000-30013.
11. Clark JC, Damaskinaki F-N, Cheung YFH, Slater A, Watson SP. Structure-function relationship of the platelet glycoprotein VI (GPVI) receptor: does it matter if it is a dimer or monomer? *Platelets*. 2021;32(6):724-732.
12. Arthur JF, Shen Y, Kahn ML, Berndt MC, Andrews RK, Gardiner EE. Ligand binding rapidly induces disulfide-dependent dimerization of glycoprotein VI on the platelet plasma membrane. *J Biol Chem*. 2007;282(42):30434-30441.
13. Billiard P, Slater A, Welin M, et al. Targeting platelet GPVI with glenzocimab: a novel mechanism for inhibition. *Blood Adv*. 2023;7(7):1258-1268.
14. Damaskinaki F-N, Jooss NJ, Martin EM, et al. Characterizing the binding of glycoprotein VI with nanobody 35 reveals a novel monomeric structure of glycoprotein VI where the conformation of D1+D2 is independent of dimerization. *J Thromb Haemost*. 2023;21(2):317-328.
15. Xu R-G, Gauer JS, Baker SR, et al. GPVI (glycoprotein VI) interaction with fibrinogen is mediated by avidity and the fibrinogen α C-region. *Arterioscler Thromb Vasc Biol*. 2021;41(3):1092-1104.
16. Mangin PH, Gardiner EE, Ariëns RA, Jandrot-Perrus M. Glycoprotein VI interplay with fibrin(ogen) in thrombosis. *J Thromb Haemost*. 2023;21(7):1703-1713.
17. Jooss NJ, Henskens YM, Watson SP, et al. Pharmacological inhibition of glycoprotein VI-and integrin α 2 β 1-induced thrombus formation modulated by the collagen type. *Thromb Haemost*. 2023;123(6):597-612.
18. Tiede C, Tang AA, Deacon SE, et al. Adhiron: a stable and versatile peptide display scaffold for molecular recognition applications. *Protein Eng Des Sel*. 2014;27(5):145-155.
19. Tiede C, Bedford R, Heseltine SJ, et al. Affimer proteins are versatile and renewable affinity reagents. *Elife*. 2017;6:e24903.

20. Robinson JI, Baxter EW, Owen RL, et al. Affimer proteins inhibit immune complex binding to FcγR11a with high specificity through competitive and allosteric modes of action. *Proc Natl Acad Sci*. 2018;115(1):E72-E81.
21. Hughes DJ, Tiede C, Penswick N, et al. Generation of specific inhibitors of SUMO-1-and SUMO-2/3-mediated protein-protein interactions using Affimer (Adhiron) technology. *Sci Signal*. 2017;10(505):eaaj2005.
22. Kyle S. Affimer proteins: theranostics of the future? *Trends Biochem Sci*. 2018;43(4):230-232.
23. Kearney KJ, Pechlivani N, King R, et al. Affimer proteins as a tool to modulate fibrinolysis, stabilize the blood clot, and reduce bleeding complications. *Blood*. 2019;133(11):1233-1244.
24. Lecut C, Feeney L, Kingsbury G, et al. Human platelet glycoprotein VI function is antagonized by monoclonal antibody-derived Fab fragments. *J Thromb Haemost*. 2003;1(12):2653-2662.
25. Nieswandt B, Brakebusch C, Bergmeier W, et al. Glycoprotein VI but not α2β1 integrin is essential for platelet interaction with collagen. *EMBO J*. 2001;20(9):2120-2130.
26. Aburima A, Berger M, Spurgeon BE, et al. Thrombospondin-1 promotes hemostasis through modulation of cAMP signaling in blood platelets. *Blood*. 2021;137(5):678-689.
27. Roberts W, Magwenzi S, Aburima A, Naseem KM. Thrombospondin-1 induces platelet activation through CD36-dependent inhibition of the cAMP/protein kinase A signaling cascade. *Blood*. 2010;116(20):4297-4306.
28. Deng B, Lento C, Wilson DJ. Hydrogen deuterium exchange mass spectrometry in biopharmaceutical discovery and development-A review. *Chem Rev*. 2016;940:8-20.
29. Honorato RV, Koukos PI, Jiménez-García B, et al. Structural biology in the clouds: the WeNMR-EOSC ecosystem. *Front Mol Biosci*. 2021;8:729513.
30. Jumper J, Evans R, Pritzel A, et al. Highly accurate protein structure prediction with AlphaFold. *Nature*. 2021;596(7873):583-589.
31. Clark JC, Neagoe RA, Zuidschermoude M, et al. Evidence that GPVI is expressed as a mixture of monomers and dimers, and that the D2 domain is not essential for GPVI activation. *Thromb Haemost*. 2021;121(11):1435-1447.
32. Poulter N, Pollitt AY, Owen D, et al. Clustering of glycoprotein VI (GPVI) dimers upon adhesion to collagen as a mechanism to regulate GPVI signaling in platelets. *J Thromb Haemost*. 2017;15(3):549-564.
33. Induruwa I, McKinney H, Kempster C, et al. Platelet surface receptor glycoprotein VI-dimer is overexpressed in stroke: the glycoprotein VI in stroke (GYPSIE) study results. *PLoS One*. 2022;17(1):e0262695.
34. Barrachina MN, Sueiro AM, Izquierdo I, et al. GPVI surface expression and signalling pathway activation are increased in platelets from obese patients: elucidating potential anti-atherothrombotic targets in obesity. *Atheroscler*. 2019;281:62-70.
35. Lecut C, Arocas V, Ulrichs H, et al. Identification of residues within human glycoprotein VI involved in the binding to collagen: evidence for the existence of distinct binding sites. *J Biol Chem*. 2004;279(50):52293-52299.
36. Jung S, Tsuji K, Moroi M. Glycoprotein (GP) VI dimer as a major collagen-binding site of native platelets: direct evidence obtained with dimeric GPVI-specific fabs. *J Thromb Haemost*. 2009;7(8):1347-1355.
37. Moroi M, Mizuguchi J, Kawashima S, et al. A new monoclonal antibody, mAb 204-11, that influences the binding of platelet GPVI to fibrous collagen. *Thromb Haemost*. 2003;89(6):996-1003.
38. Michel MA, Swatek KN, Hospenthal MK, Komander DJMc. Ubiquitin linkage-specific affimers reveal insights into K6-linked ubiquitin signaling. *Mol Cell*. 2017;68(1):233-246.e5.
39. Ye Y, Blaser G, Horrocks MH, et al. Ubiquitin chain conformation regulates recognition and activity of interacting proteins. *Nature*. 2012;492(7428):266-270.